



Published in final edited form as:

*Antiviral Res.* 2017 August ; 144: 147–152. doi:10.1016/j.antiviral.2017.06.011.

## 4'-Azidocytidine (R1479) inhibits henipaviruses and other paramyxoviruses with high potency

Anne L. Hotard<sup>a</sup>, Biao He<sup>b</sup>, Stuart T. Nichol<sup>a</sup>, Christina F. Spiropoulou<sup>a,\*\*</sup>, and Michael K. Lo<sup>a,\*</sup>

<sup>a</sup>Viral Special Pathogens Branch, Centers for Disease Control and Prevention, Atlanta, GA, USA

<sup>b</sup>Department of Infectious Diseases, College of Veterinary Medicine, University of Georgia, Athens, GA, USA

### Abstract

The henipaviruses Nipah virus and Hendra virus are highly pathogenic zoonotic paramyxoviruses which have caused fatal outbreaks of encephalitis and respiratory disease in humans. Despite the availability of a licensed equine Hendra virus vaccine and a neutralizing monoclonal antibody shown to be efficacious against henipavirus infections in non-human primates, there remains no approved therapeutics or vaccines for human use. To explore the possibility of developing small-molecule nucleoside inhibitors against henipaviruses, we evaluated the antiviral activity of 4'-azidocytidine (R1479), a drug previously identified to inhibit flaviviruses, against henipaviruses along with other representative members of the family *Paramyxoviridae*. We observed similar levels of R1479 antiviral activity across the family, regardless of virus genus. Our brief study expands the documented range of viruses susceptible to R1479, and provides the basis for future investigation and development of 4'-modified nucleoside analogs as potential broad-spectrum antiviral therapeutics across both positive and negative-sense RNA virus families.

### Keywords

Henipavirus; Nipah virus; Nucleoside analog; Antiviral 4'-Azidocytidine

Nipah virus (NiV) and Hendra virus (HeV) are the highly pathogenic, prototype members of the Henipavirus genus in the *Paramyxoviridae* family (Rota and Lo, 2012). While there is an approved animal vaccine against equine Hendra virus infections and a monoclonal antibody that is efficacious against henipavirus infection in non-human primates (Geisbert et al., 2014; Peel et al., 2016), there are no small-molecule antiviral therapeutics which have proven effective at inhibiting NiV and HeV both *in vitro* and *in vivo* (Mathieu and Horvat, 2015). Recently, several small-molecules, including a nucleotide analog, have shown promise *in vitro*, but remain to be tested *in vivo* (Lo et al., 2017; Mohr et al., 2015). Given the paucity of small-molecule therapeutics targeting these highly pathogenic viruses, we began exploring the susceptibility of henipaviruses and other related paramyxoviruses to relatively well-characterized and commercially available nucleoside analogs, one of which

\*Corresponding author. 1600 Clifton Road, Mailstop G-14, Atlanta, GA, 30333, USA. \*\*Corresponding author. 1600 Clifton Road, Mailstop G-14, Atlanta, GA, 30333, USA.

was 4'-azidocytidine (R1479). R1479 is the major circulating form of the tri-isobutyl ester prodrug balapiravir in plasma, and was initially identified as a potent *in vitro* inhibitor of a hepatitis C virus (HCV) replicon in the mid-2000s (50% effective inhibitory concentration (EC<sub>50</sub>): 1.28 μM) (Klumpp et al., 2006). Since then, R1479 was shown to inhibit the RNA-dependent RNA polymerase (RdRP) activities of Dengue virus (DenV) (EC<sub>50</sub>: 1.9–11 μM) and respiratory syncytial virus (RSV) (EC<sub>50</sub>: 0.24 μM) (Nguyen et al., 2013; Wang et al., 2015). The pro-drug balapiravir advanced to clinical trials for HCV and DenV, but these trials were discontinued due to adverse toxicity reactions and lack of efficacy (Nelson et al., 2012; Nguyen et al., 2013; Roberts et al., 2008). The depotentiation of balapiravir due to DenV activation of immune cells may explain the discordance of the *in vitro* data with the *in vivo* results (Chen et al., 2014).

Despite the results from clinical trials utilizing balapiravir, further characterization of compounds structurally similar to R1479 yielded other potential inhibitors of both HCV and RSV (Deval et al., 2015; Jordan et al., 2017; Smith et al., 2009; Wang et al., 2015). Results from these studies highlighted the importance of investigating structure-activity relationships regarding the modifications that afforded nucleoside analogs optimal antiviral activity. Since R1479 was shown to inhibit RdRP activity of RSV, we elected to investigate whether R1479 would show activity against henipaviruses. Due to the conservation of RdRP binding domain structure across multiple virus families (Lo et al., 2017), we expected R1479 to effectively inhibit NiV and HeV, and to serve as a frame of reference for exploring the antiviral activity of other 4'-modified nucleoside analogs. The wild type NiV and HeV used in this study were from the Centers for Disease Control and Prevention (CDC) Viral Special Pathogens reference collection, and all experiments with wild type or recombinant NiV and HeV were performed in the CDC Biosafety Level 4 High Containment Laboratory.

We first assayed the ability of R1479 to inhibit reporter activity from recombinant GFP- or luciferase-expressing NiVs (Lo et al., 2014). For these assays,  $2 \times 10^4$  NCI-H358 bronchioalveolar carcinoma epithelial cells (CRL-5807, ATCC, Manassas, VA, USA) seeded in opaque 96-well plates were treated with 2-fold serial dilutions of R1479 (starting concentration 100 μM; Carbosynth US LLC, San Diego, CA, USA) for 1 h prior to infection with NiV-Luc2AM or NiV-GFP2AM at multiplicity of infection (MOI) 0.2. Infected cells were incubated continually in the presence of R1479 for the duration of each assay. Twenty-four (NiV-Luc2AM) or 72 (NiV-GFP2AM) hours post infection (hpi), reporter activity was quantified and 50% effective inhibitory concentrations (EC<sub>50</sub>) were calculated from dose-response data fitted to a 4-parameter logistic curve (Graph-Pad Prism, La Jolla, CA, USA). Fig. 1A and B are dose-response curves representative of at least 4 biological replicates across at least 2 replicate experiments using NiV-Luc2AM and NiV-GFP2AM, respectively. Mean R1479 EC<sub>50</sub> values are denoted in Table 1, and were less than 2 μM against both reporter NiVs. NiV and HeV infections result in striking cytopathic effect (CPE) in cells which is quantifiable by a reduction in cell viability, as measured using CellTiter-Glo 2.0 reagent (Promega, Madison, WI, USA). Utilizing an assay described previously (Flint et al., 2014; Tigabu et al., 2014), we measured the ability of R1479 to inhibit wild type NiV (Malaysia genotype) and HeV-induced CPE at 72 hpi in NCI-H358 cells (Fig. 1C and D). In this CPE inhibition assay, the mean R1479 EC<sub>50</sub> was 2.63 μM against NiV and 1.75 μM against HeV (Table 1). We performed the NiV-Luc2AM and CPE assays in HeLa cells, and

determined mean EC<sub>50</sub> values against NiV and HeV to be approximately 5-fold higher in each assay (Table 1). The difference in EC<sub>50</sub> values between the two cell lines may be due to a differential ability to metabolize R1479 into the fully active, triphosphate form.

While outbreaks of henipavirus infection in humans have the highest mortality rate compared to outbreaks of other paramyxoviruses, they are less common and affect fewer people overall (Mathieu and Horvat, 2015). To define the potential of R1479 to inhibit viruses across the *Paramyxoviridae* family, we also measured its activity against a representative morbillivirus (measles virus, MV, rMV<sup>EZ</sup>GFP(3)), respirovirus (human parainfluenza virus 3, hPIV3, hPIV3-GFP), and rubulavirus (mumps virus, MuV, rMuV-EGFP). Since each virus employed expresses GFP (Rennick et al., 2015; Xu et al., 2011; Zhang et al., 2005), we measured the ability of R1479 to inhibit infection-induced GFP expression. For rMV<sup>EZ</sup>GFP(3) and hPIV3-GFP, we infected NCI-H358 cells at MOI 1.0 and 2.0 respectively, after treating cells with serial dilutions of R1479 for approximately 1 h. We quantified total GFP fluorescence 72 hpi and determined EC<sub>50</sub> values as described above for NiV-GFP2AM. Mean R1479 EC<sub>50</sub> values against both viruses were only marginally higher than those quantified for the henipaviruses (Fig. 1E and F, Table 1). We infected R1479-treated NCI-H358 cells with rMuV-EGFP at MOI 0.5 for 7 days, at which point GFP positive cells were counted using a Biotek Cytation 5 plate reader (Biotek, Winooski, VT, USA). The average number of background cell counts were subtracted from each well to give normalized cells counts, and any negative values were adjusted to “0”. For analysis of each replicate, the highest number of positive counts was regarded as 100%, while 0 counts was used for 0% positivity. Following this normalization, data were fitted to a 4-parameter logistic curve. A representative curve is shown in Fig. 1G, and the mean EC<sub>50</sub> value from multiple replicates was determined to be 5.48 μM (Table 1). Taken together, our data demonstrate the potent antiviral activity of R1479 across the *Paramyxoviridae* family.

Previous publications report a sub-micromolar EC<sub>50</sub> value of R1479 against the *Pneumovirus* RSV (Deval et al., 2015; Wang et al., 2015). We used a GFP-expressing recombinant RSV (rgRSV224) (Hallak et al., 2000) to confirm these findings. In NCI-H358 cells, we measured a mean EC<sub>50</sub> against RSV to be 4.35 μM (Fig. 1E, Table 1). This difference relative to published data is likely due to differences in the assays used. In the previous reports, either a subgenomic replicon or purified polymerase complex extract was tested for inhibition by R1479, while we measured activity against live virus in infected cells. Our data with RSV is similar to our data for the paramyxoviruses, which is expected given the genetic relatedness and similar replication mechanisms shared by paramyxo- and pneumoviruses. Given the observed broad spectrum activity of R1479, we evaluated its activity against a recombinant reporter Rift Valley Fever virus (RVFV) (Bird et al., 2008), and found no antiviral activity (Fig. 1I).

To further characterize the inhibition of henipaviruses by R1479, we performed immunofluorescence assays on NCI-H358 cells treated with R1479 and infected with wild type NiV. Seventy-two hours post-infection, cells were fixed and stained with a monoclonal antibody against the NiV nucleoprotein (Chiang et al., 2010). Fluorescence was detected using a DyLight 488-conjugated secondary antibody (Bethyl Laboratories, Montgomery, TX, USA), and cells were counterstained with 4',6-diamidino-2-phenylindole (DAPI;

Invitrogen, Carlsbad, CA, USA). We captured fluorescence images at 10× magnification using a Nikon Eclipse Ti inverted fluorescence microscope (Nikon, Melville, NY, USA). The observed numbers of fluorescent syncytia indicative of Henipavirus replication and CPE inversely correlated with concentrations of R1479 in a dose-dependent manner (Fig. 2), correlating with the results from our NiV luciferase, GFP, and CPE assays in Fig. 1.

As a final measure of R1479 activity against NiV and HeV, we performed virus titer reduction (VTR) assays with each wild type virus in NCI-H358 cells. Here, NiV or HeV was adsorbed to cells at MOI = 0.2 for 1 h at 37 °C. Following this incubation, inoculum was removed from cells, cells were washed with PBS, and media containing 2-fold serial dilutions of R1479 was added to cells. Each infection/R1479 dilution was performed in quadruplicate. Supernatants were removed 48 hpi and frozen at –80 °C until 50% tissue culture infectious dose (TCID<sub>50</sub>) was quantified in Vero cells (8 wells per dilution). Four days post-infection, Vero cells were visually assayed for CPE and endpoint virus titers were calculated using the Reed and Muench method (Reed and Muench, 1938). Fig. 3 shows the titer reduction curves and R1479 EC<sub>50</sub> values for NiV (Fig. 3, panel A) and HeV (Fig. 3, panel B). As with the assays displayed in Fig. 1, R1479 EC<sub>50</sub> values in the VTR assays against NiV and HeV were low micromolar concentrations (1.53 μM and 2.41 μM, respectively). We also performed VTR assays in HeLa cells for both NiV and HeV, and while the EC<sub>50</sub> values were similar to those obtained from NCI-H358 cells, R1479 was only able to reduce infectious virus titer by more than 2 orders of magnitude only at the highest concentrations used (50, 100 μM) (Table 1, data not shown). These data confirm our earlier findings that R1479 is potent against henipaviruses in NCI-H358 cells.

Our results from multiple assay types show that R1479 shows efficacy against henipaviruses with low micromolar EC<sub>50</sub> values, and has minimal cellular cytotoxicity (CC<sub>50</sub> > 100 μM) (Fig. 1J, Table 1). Slight differences in EC<sub>50</sub> values between assays are expected due to the differing sensitivities inherent to the assays. We found similar EC<sub>50</sub> values for R1479 against other paramyxoviruses as well, indicating that R1479 not only has potent antiviral activity across the *Paramyxoviridae*, but that the levels of potency documented closely parallel those observed for R1479 against Flaviviruses and a Pneumovirus (Chen et al., 2014; Eyer et al., 2016; Klumpp et al., 2006; Smith et al., 2007; Wang et al., 2015). Also of note, we found that R1479 exhibited an approximate five-fold increase in EC<sub>50</sub> values when tested against viruses in HeLa cells as compared to NCI-H358 cells. The likely difference in ability of the two cell types to convert R1479 to the fully active, triphosphorylated form underscores the need for testing multiple cell lines when evaluating any small molecule for antiviral activity. In this study, we presumed that the antiviral activity of R1479 observed against the panel of paramyxoviruses in this study was due to R1479 acting as an RNA chain terminator, as was shown for RSV (Wang et al., 2015). Future development of *in vitro* polymerase assays for paramyxoviruses will serve as useful tools not only to evaluate and confirm the activity of nucleoside analogs, but to better elucidate the enzymatic and structural characteristics of paramyxovirus polymerase complexes. Although neither R1479 nor its prodrug balapiravir are likely to advance as antiviral therapeutics due to poor bioavailability and previous clinical trial results, our data indicate that 4'-modified nucleosides can serve as a basis for developing a broad-spectrum antiviral therapeutic with near-equivalent potencies across positive and negative-sense RNA virus families. The breadth of R1479 activity observed in

this study against paramyxoviruses and a pneumovirus indicates that other families within the order *Mononegavirales* may also be susceptible to inhibition by R1479. These results, along with recent advances in broad-spectrum antiviral screening techniques (Yan et al., 2013), and new tools for high-throughput screening against highly pathogenic viruses (Albarino et al., 2013, 2015; Lo et al., 2014; Welch et al., 2016) highlight the potential and the utility for both discovering new antiviral drugs and repurposing existing ones to combat viral diseases with global public health implications.

## Acknowledgments

The findings and conclusions in this report are those of the authors and do not necessarily represent those of the Centers for Disease Control and Prevention. This work was financially supported by CDC core funding. ALH was sponsored by the American Society for Microbiology/Centers for Disease Control and Prevention Postdoctoral Fellowship.

## References

- Albarino CG, Uebelhoefer LS, Vincent JP, Khristova ML, Chakrabarti AK, McElroy A, Nichol ST, Towner JS. Development of a reverse genetics system to generate recombinant Marburg virus derived from a bat isolate. *Virology*. 2013; 446:230–237. [PubMed: 24074586]
- Albarino CG, Wiggleson Guerrero L, Lo MK, Nichol ST, Towner JS. Development of a reverse genetics system to generate a recombinant Ebola virus Makona expressing a green fluorescent protein. *Virology*. 2015; 484:259–264. [PubMed: 26122472]
- Bird BH, Albarino CG, Hartman AL, Erickson BR, Ksiazek TG, Nichol ST. Rift valley fever virus lacking the NSs and NSm genes is highly attenuated, confers protective immunity from virulent virus challenge, and allows for differential identification of infected and vaccinated animals. *J Virol*. 2008; 82:2681–2691. [PubMed: 18199647]
- Chen YL, Abdul Ghafar N, Karuna R, Fu Y, Lim SP, Schul W, Gu F, Herve M, Yokohama F, Wang G, Cerny D, Fink K, Blasco F, Shi PY. Activation of peripheral blood mononuclear cells by dengue virus infection depotentiates balapiravir. *J Virol*. 2014; 88:1740–1747. [PubMed: 24257621]
- Chiang CF, Lo MK, Rota PA, Spiropoulou CF, Rollin PE. Use of mono-clonal antibodies against Hendra and Nipah viruses in an antigen capture ELISA. *Virol J*. 2010; 7:115. [PubMed: 20525276]
- Deval J, Hong J, Wang G, Taylor J, Smith LK, Fung A, Stevens SK, Liu H, Jin Z, Dyatkina N, Prhac M, Stoycheva AD, Serebryany V, Liu J, Smith DB, Tam Y, Zhang Q, Moore ML, Fearn R, Chanda SM, Blatt LM, Symons JA, Beigelman L. Molecular basis for the selective inhibition of respiratory syncytial virus RNA polymerase by 2'-fluoro-4'-chloromethyl-cytidine triphosphate. *PLoS Pathog*. 2015; 11:e1004995. [PubMed: 26098424]
- Eyer L, Smidkova M, Nencka R, Neca J, Kastl T, Palus M, De Clercq E, Ruzek D. Structure-activity relationships of nucleoside analogues for inhibition of tick-borne encephalitis virus. *Antivir Res*. 2016; 133:119–129. [PubMed: 27476046]
- Flint M, McMullan LK, Dodd KA, Bird BH, Khristova ML, Nichol ST, Spiropoulou CF. Inhibitors of the tick-borne, hemorrhagic fever-associated flaviviruses. *Antimicrob Agents Chemother*. 2014; 58:3206–3216. [PubMed: 24663025]
- Geisbert TW, Mire CE, Geisbert JB, Chan YP, Agans KN, Feldmann F, Fenton KA, Zhu Z, Dimitrov DS, Scott DP, Bossart KN, Feldmann H, Broder CC. Therapeutic treatment of Nipah virus infection in nonhuman primates with a neutralizing human monoclonal antibody. *Sci Transl Med*. 2014; 6:242ra282.
- Hallak LK, Spillmann D, Collins PL, Peeples ME. Glycosaminoglycan sulfation requirements for respiratory syncytial virus infection. *J Virol*. 2000; 74:10508–10513. [PubMed: 11044095]
- Jordan PC, Stevens SK, Tam Y, Pemberton RP, Chaudhuri S, Stoycheva AD, Dyatkina N, Wang G, Symons JA, Deval J, Beigelman L. Activation pathway of a nucleoside analog inhibiting respiratory syncytial virus polymerase. *ACS Chem Biol*. 2017; 12:83–91. [PubMed: 28103684]

- Klumpp K, Leveque V, Le Pogam S, Ma H, Jiang WR, Kang H, Granycome C, Singer M, Laxton C, Hang JQ, Sarma K, Smith DB, Heindl D, Hobbs CJ, Merrett JH, Symons J, Cammack N, Martin JA, Devos R, Najera I. The novel nucleoside analog R1479 (4'-azidocytidine) is a potent inhibitor of NS5B-dependent RNA synthesis and hepatitis C virus replication in cell culture. *J Biol Chem.* 2006; 281:3793–3799. [PubMed: 16316989]
- Lo MK, Jordan R, Arvey A, Sudhamsu J, Shrivastava-Ranjan P, Hotard AL, Flint M, McMullan LK, Siegel D, Clarke MO, Mackman RL, Hui HC, Perron M, Ray AS, Cihlar T, Nichol ST, Spiropoulou CF. GS-5734 and its parent nucleoside analog inhibit Filo-, Pneumo-, and Paramyxoviruses. *Sci Rep.* 2017; 7:43395. [PubMed: 28262699]
- Lo MK, Nichol ST, Spiropoulou CF. Evaluation of luciferase and GFP-expressing Nipah viruses for rapid quantitative antiviral screening. *Antivir Res.* 2014; 106:53–60. [PubMed: 24680955]
- Mathieu C, Horvat B. Henipavirus pathogenesis and antiviral approaches. *Expert Rev Anti Infect Ther.* 2015; 13:343–354. [PubMed: 25634624]
- Mohr EL, McMullan LK, Lo MK, Spengler JR, Bergeron E, Albarino CG, Shrivastava-Ranjan P, Chiang CF, Nichol ST, Spiropoulou CF, Flint M. Inhibitors of cellular kinases with broad-spectrum antiviral activity for hemorrhagic fever viruses. *Antivir Res.* 2015; 120:40–47. [PubMed: 25986249]
- Nelson DR, Zeuzem S, Andreone P, Ferenci P, Herring R, Jensen DM, Marcellin P, Pockros PJ, Rodriguez-Torres M, Rossaro L, Rustgi VK, Sepe T, Sulkowski M, Thomason IR, Yoshida EM, Chan A, Hill G. Balapiravir plus peginterferon alfa-2a (40KD)/ribavirin in a randomized trial of hepatitis C genotype 1 patients. *Ann Hepatol.* 2012; 11:15–31. [PubMed: 22166557]
- Nguyen NM, Tran CN, Phung LK, Duong KT, Huynh Hle A, Farrar J, Nguyen QT, Tran HT, Nguyen CV, Merson L, Hoang LT, Hibberd ML, Aw PP, Wilm A, Nagarajan N, Nguyen DT, Pham MP, Nguyen TT, Javanbakht H, Klumpp K, Hammond J, Petric R, Wolbers M, Nguyen CT, Simmons CP. A randomized, double-blind placebo controlled trial of balapiravir, a polymerase inhibitor, in adult dengue patients. *J Infect Dis.* 2013; 207:1442–1450. [PubMed: 22807519]
- Peel AJ, Field HE, Reid PA, Plowright RK, Broder CC, Skerratt LF, Hayman DT, Restif O, Taylor M, Martin G, Crameri G, Smith I, Baker M, Marsh GA, Barr J, Breed AC, Wood JL, Dhand N, Toribio JA, Cunningham AA, Fulton I, Bryden WL, Secombe C, Wang LF. The equine Hendra virus vaccine remains a highly effective preventative measure against infection in horses and humans: 'The imperative to develop a human vaccine for the Hendra virus in Australia'. *Infect Ecol Epidemiol.* 2016; 6:31658. [PubMed: 27151273]
- Reed L, Muench H. A simple method of estimating fifty percent endpoints. *Am J Hyg.* 1938; 27:493–497.
- Rennick LJ, de Vries RD, Carsillo TJ, Lemon K, van Amerongen G, Ludlow M, Nguyen DT, Yuksel S, Verburgh RJ, Haddock P, McQuaid S, Duprex WP, de Swart RL. Live-attenuated measles virus vaccine targets dendritic cells and macrophages in muscle of nonhuman primates. *J Virol.* 2015; 89:2192–2200. [PubMed: 25473055]
- Roberts SK, Cooksley G, Dore GJ, Robson R, Shaw D, Berns H, Hill G, Klumpp K, Najera I, Washington C. Robust antiviral activity of R1626, a novel nucleoside analog: a randomized, placebo-controlled study in patients with chronic hepatitis C. *Hepatology.* 2008; 48:398–406. [PubMed: 18553458]
- Rota PA, Lo MK. Molecular virology of the henipaviruses. *Curr Top Microbiol Immunol.* 2012; 359:41–58. [PubMed: 22552699]
- Smith DB, Kalayanov G, Sund C, Winqvist A, Maltseva T, Leveque VJ, Rajyaguru S, Le Pogam S, Najera I, Benkestock K, Zhou XX, Kaiser AC, Maag H, Cammack N, Martin JA, Swallow S, Johansson NG, Klumpp K, Smith M. The design, synthesis, and antiviral activity of monofluoro and difluoro analogues of 4'-azidocytidine against hepatitis C virus replication: the discovery of 4'-azido-2'-deoxy-2'-fluorocytidine and 4'-azido-2'-dideoxy-2',2'-difluorocytidine. *J Med Chem.* 2009; 52:2971–2978. [PubMed: 19341305]
- Smith DB, Martin JA, Klumpp K, Baker SJ, Blomgren PA, Devos R, Granycome C, Hang J, Hobbs CJ, Jiang WR, Laxton C, Le Pogam S, Leveque V, Ma H, Maile G, Merrett JH, Pichota A, Sarma K, Smith M, Swallow S, Symons J, Vesey D, Najera I, Cammack N. Design, synthesis, and antiviral properties of 4'-substituted ribonucleosides as inhibitors of hepatitis C virus replication: the discovery of R1479. *Bioorg Med Chem Lett.* 2007; 17:2570–2576. [PubMed: 17317178]

- Tigabu B, Rasmussen L, White EL, Tower N, Saeed M, Bukreyev A, Rockx B, LeDuc JW, Noah JW. A BSL-4 high-throughput screen identifies sulfonamide inhibitors of Nipah virus. *Assay Drug Dev Technol.* 2014; 12:155–161. [PubMed: 24735442]
- Wang G, Deval J, Hong J, Dyatkina N, Prhac M, Taylor J, Fung A, Jin Z, Stevens SK, Serebryany V, Liu J, Zhang Q, Tam Y, Chanda SM, Smith DB, Symons JA, Blatt LM, Beigelman L. Discovery of 4'-chloromethyl-2'-deoxy-3',5'-di-O-isobutyryl-2'-fluorocytidine (ALS-8176), a first-in-class RSV polymerase inhibitor for treatment of human respiratory syncytial virus infection. *J Med Chem.* 2015; 58:1862–1878. [PubMed: 25667954]
- Welch SR, Guerrero LW, Chakrabarti AK, McMullan LK, Flint M, Bluemling GR, Painter GR, Nichol ST, Spiropoulou CF, Albarino CG. Lassa and Ebola virus inhibitors identified using minigenome and recombinant virus reporter systems. *Antivir Res.* 2016; 136:9–18. [PubMed: 27771389]
- Xu P, Li Z, Sun D, Lin Y, Wu J, Rota PA, He B. Rescue of wild-type mumps virus from a strain associated with recent outbreaks helps to define the role of the SH ORF in the pathogenesis of mumps virus. *Virology.* 2011; 417:126–136. [PubMed: 21676427]
- Yan D, Krumm SA, Sun A, Steinhauer DA, Luo M, Moore ML, Plemper RK. Dual myxovirus screen identifies a small-molecule agonist of the host antiviral response. *J Virol.* 2013; 87:11076–11087. [PubMed: 23926334]
- Zhang L, Bukreyev A, Thompson CI, Watson B, Peeples ME, Collins PL, Pickles RJ. Infection of ciliated cells by human parainfluenza virus type 3 in an in vitro model of human airway epithelium. *J Virol.* 2005; 79:1113–1124. [PubMed: 15613339]

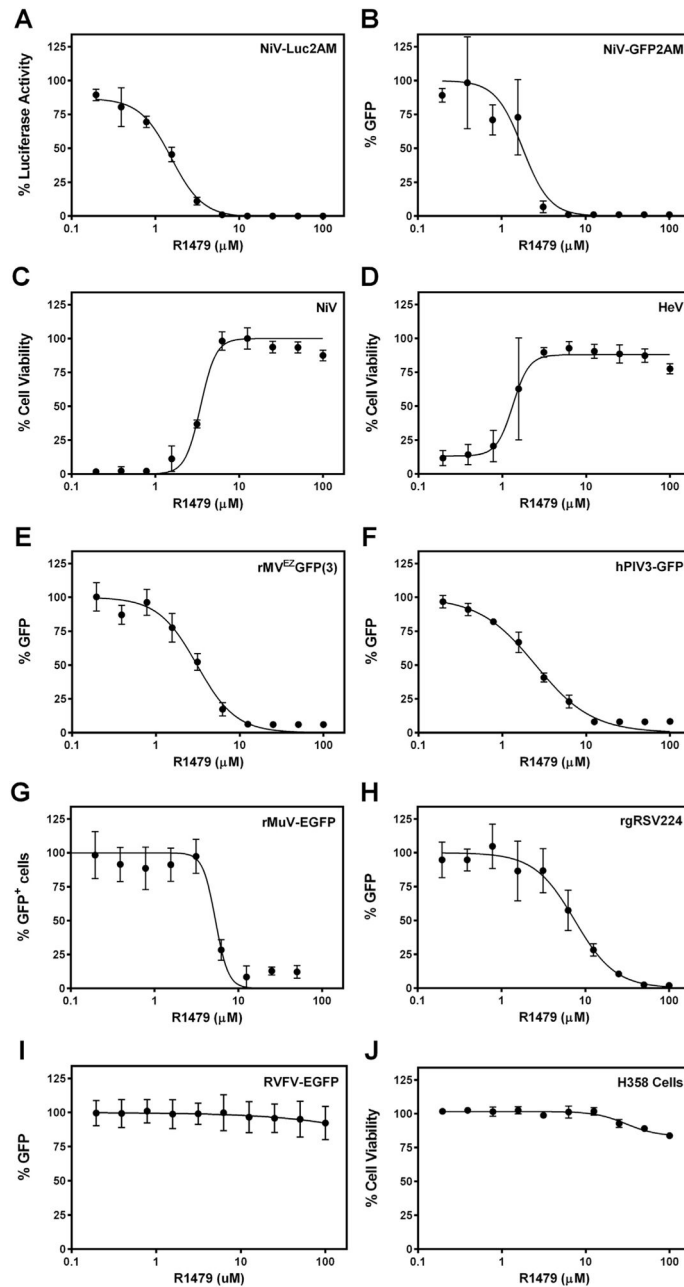


**Fig. 1.**

Antiviral activity of R1479 against multiple paramyxoviruses. Representative dose-response curves for various antiviral assays using R1479 in NCI-H358 cells. (A) Luciferase activity 24 hpi with NiV-Luc2AM. (B) Total GFP positivity as a percentage of DMSO treatment control, quantified 72 hpi with NiV-GFP2AM. (C and D) Cell viability measured by CellTiter-Glo 2.0 72 hpi with wild type NiV (C) or HeV (D). (E, F, G, H, and I) Total GFP positivity as a percentage of no R1479 of rMV<sup>EZ</sup>-GFP(3) (E), hPIV3-GFP (F), rMuV-EGFP (G), rgRSV224 (H), or RVFV-EGFP (I) quantified at 72 hpi. For (G), the number of GFP positive cells was counted and reported as percentage of number of GFP positive cells in no



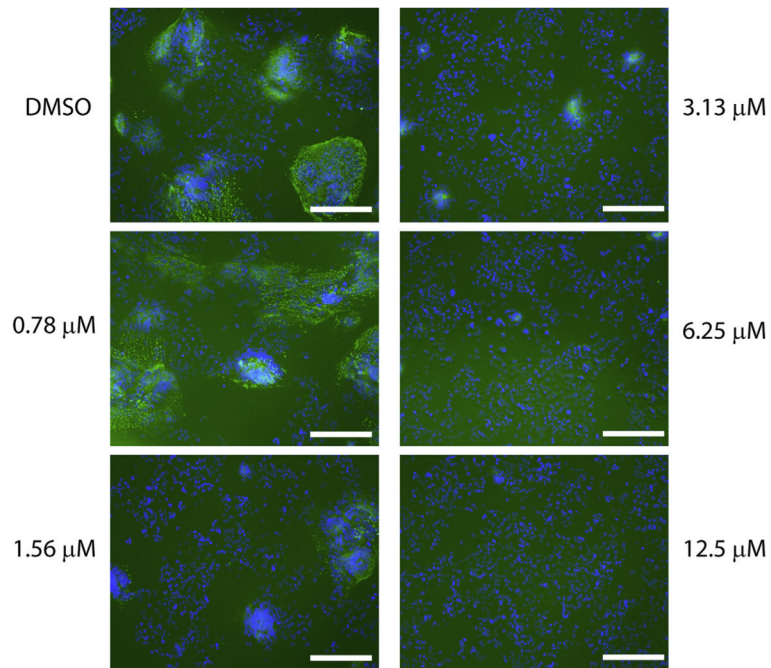
R1479 control. (J) Cell viability as percentage of DMSO treatment control in uninfected NCI-H358 cells incubated for 72 h post-R1479 treatment. All curves are representative of at least 4 biological replicates across at least 2 experiments.

Author Manuscript

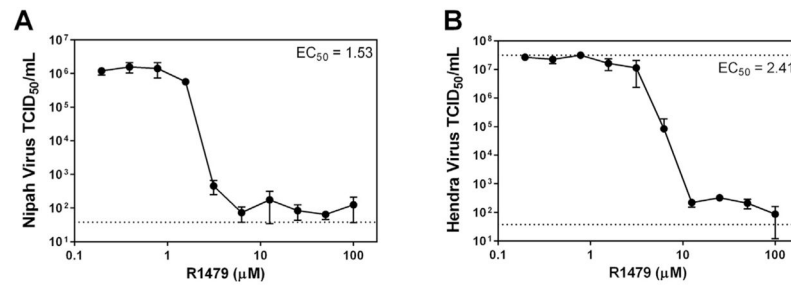
Author Manuscript

Author Manuscript

Author Manuscript



**Fig. 2.** Immunofluorescence microscopy of wild type NiV-infected, R1479 treated cells. NCI-H358 cells pretreated with 2-fold serial dilutions of R1479 were infected with wild type NiV at MOI 0.2 for 72 h. Cells were then fixed, permeabilized, and stained with a mouse monoclonal antibody against NiV nucleoprotein and a DyLight 488-conjugated donkey anti-mouse secondary antibody (green). Cells were counterstained with DAPI (blue), and representative images were captured at 10× magnification. White bar indicates length of 100 μm.

**Fig. 3.**

Virus titer reduction assay. NCI-H358 cells were infected with MOI 0.2 of wild type NiV (A) or HeV (B) for 1 h at 37 °C. After 1 h incubation, virus inocula were removed, cells were washed in PBS, and media containing 2-fold serial dilutions of R1479 was added to cells. Cells were allowed to incubate for 48 h, at which time supernatant was removed and used to determine TCID<sub>50</sub> on Vero cells. Each experiment was performed in quadruplicate, and the calculated EC<sub>50</sub> values are displayed. The dotted line at 37.7 TCID<sub>50</sub>/mL is the lower limit of detection, and the dotted line at  $3.16 \times 10^7$  TCID<sub>50</sub>/mL is the upper limit of detection.

Table 1

Summary of R1479 results.

Virus	Assay	Cell Line	EC <sub>50</sub> (μM) <sup>a</sup>	CC <sub>50</sub> (μM)	SI
NIV	Luc	NCI-H358	1.12 ± 0.25	>100	>89
		HeLa	5.68 ± 1.91	>100	>17
	GFP	NCI-H358	1.64 ± 0.42	>100	>60
		NCI-H358	2.63 ± 0.83	>100	>38
	WT (CPE)	HeLa	13.55 ± 0.35	>100	>7
		NCI-H358	1.53	>100	>65
HeV	WT (CPE)	HeLa	4.00	>100	>25
		NCI-H358	1.75 ± 0.26	>100	>57
	WT (VTR)	HeLa	9.84 ± 0.97	>100	>10
		NCI-H358	2.41	>100	>41
	WT (VTR)	HeLa	2.25	>100	>44
		NCI-H358	3.24 ± 1.28	>100	>30
MV (rMV <sup>EGFP</sup> (3))	GFP	2.70 ± 1.06	>100	>37	
hPIV3 (hPIV3-GFP)	GFP	5.48 ± 0.42	>100	>18	
MuV (rMuV-EGFP)	GFP	4.35 ± 2.47	>100	>22	
RSV (rgRSV224)	GFP	>100	>100	ND	
RVFV (RVFV-EGFP)	GFP	>100	>100	ND	

EC<sub>50</sub> values for R1479 against each virus in all assays performed. Selectivity Index (SI) is EC<sub>50</sub>/CC<sub>50</sub>.<sup>a</sup>For all assays except VTR, mean ± standard deviations of results from at least 3 biological replicates spanning at least 2 experiments. VTR assay results denote the mean from 4 biological replicates in a single experiment. ND: not determined.